Cohesive zone model for hydrogen embrittlement in intergranular fracture and slow crack growth in Al 5xxx/7xxx alloys

N. Benali,[1,2] *R. Estevez*[1], *D. Tanguy*[2], *D. Delafosse*[2]
[1] *Université de Lyon, Insa-Lyon, MATEIS CNRS UMR 5510, France*
[2] *Centre SMS, Ecole des Mines de Saint-Etienne, France*

The aluminium alloys of the series 5xxx or 7xxx are prone to a heterogeneous precipitation along the grain boundaries which results in a heterogeneous hydrogen embrittlement. The presence of H weakens the interface along the precipitates while the 'natural' ligaments remain safe. We first analyse the decohesion process of such heterogeneous grain boundary and try to get insight on the peak for the corrosion observed for precipitates about 50nm long. We then define an 'average' cohesive model that mimics the influence of the hydrogen along a homogenised grain boundary with a decrease of cohesion energy with the concentration of H. A 2D polycrystal exhibiting intergranular failure is considered and loaded under mode I to analyse the condition for slow crack growth. We investigate how the presence of initial stresses issued from a predeformation are necessary for crack propagation. Monotonic, fatigue and applied constant loads are considered.

1. Introduction

The aluminium alloys of the 5xxx series can be susceptible to stress corrosion cracking (SCC) when immersed in an aqueous environment. Crack propagation involves the anodic dissolution of the Al_3Mg_2 compounds along the grain boundaries and also the embrittlement of the interface between these precipitates and the matrix [1], ahead of the crack tip, due to H trapping. Hydrogen is produced within the crack by the anodic dissolution. The susceptibility to SCC and H embrittlement exhibits a strong dependence with the size and distribution of the intergranular precipitates.
The peak sensibility is obtained when the precipitation is so called 'continuous'. In fact, the apparent 'continuity' stems from the observation of densely distributed lens shaped precipitates (50 nm long / 8 nm wide), in TEM. It appears that 5xxx alloys are very resistant to crack initiation after a solution heat treatment or when the precipitates are globulized when overaged. The role of H in the failure of grain boundaries has been studied in depth in the 7xxx series where trapping of H at the $MgZn_2$ intergranular precipitates, more precisely at the matrix-precipitates interface, has been directly observed [1]. However, the grain boundary in between these tiny precipitates is expected to be a weak trap for H. How does the failure take place along such heterogeneous interface and how the precipitates size effects arise remains to be clarified.

In a first part, the present study aims at gaining insight on the micromechanics of the failure process by comparing a precipitate free interface with heterogeneous

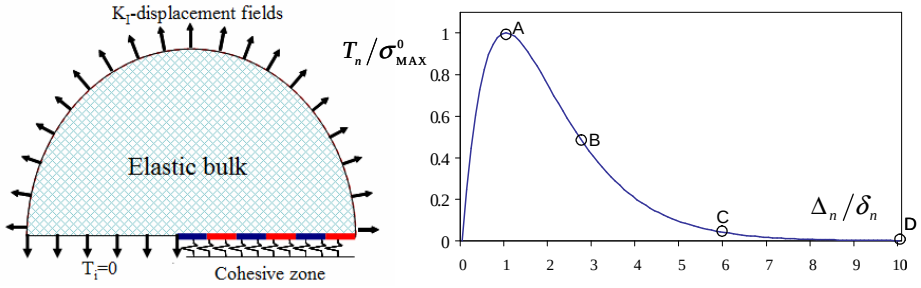

(a) (b)

Fig. 1. (a) the small scale yielding problem with a linear elastic, isotropic bulk and a cohesive zone interface along the crack symmetry plane. (b) The variation of the traction-opening cohesive zone adopted in the description. Different σ_{max}^{0} are considered for a heterogeneous interface, plain-blue and line-red domains in (a).

interfaces of various sizes of precipitates. We examine how a heterogeneous hydrogen embrittlement of the magnesium precipitates could weaken the grain boundary. To the end, we analyse the conditions for crack propagation along a heterogeneous interface inserted in between two elastic bulks, where a crack emerges. The heterogeneous interface for the grain boundary consists in safe domains and others when hydrogen can be trapped resulting in a progressive reduction of the cohesive strength. We investigate the resulting strength variation of the grain boundary and how this could assist failure. Then, we define an effective, equivalent, cohesive zone representing the failure of heterogeneous interface and finally, sketch the analysis of failure in a 2D polycrystal.

2. A basic analysis of the intergranular decohesion

In order to assess the influence of a heterogeneous weakening along a grain boundary, we consider a simplified configuration made of a heterogeneous interface inserted into two linear isotropic elastic blocks and subjected to a mode I loading. The loading conditions are represented schematically in Fig. 1a. We analyse a mode I fracture process under plane strain conditions. Small scale yielding is assumed and a boundary layer approach is adopted that results in prescribing the displacement K_I-fields along the outer circle. A natural crack is considered with a traction free face.

Cohesive zones are laid down along the crack symmetry plane, along the location of the maximum principal stress. In the case of a homogeneous problem, the cohesive zone properties are uniform along the interface with the traction-opening displacement reported in Fig. 1b, borrowed from Needleman [2,3]. The variation of the traction-opening cohesive surface shows a maximum (see Fig. 1b) for (A) $T_n = \sigma_{max}^{0}$, followed by progressive debonding with $T_n = \sigma_{max}^{0}/2$ at (B) up to the onset of crack propagation at (C). The area under the T_n-Δ_n plot corresponds to the work of separation Φ_{SEP} = exp(1). $\sigma_{max}^{0}\delta_n$, with σ_{max}^{0} and δ_n being material parameters related to the properties of the interface. For the case of a homogeneous interface representative of an unbrittled, hydrogen free, interface we have considered σ_{max}^{0}= 1GPa and δ_n=1nm resulting in Φ_{SEP}=2.7J/m^2. By

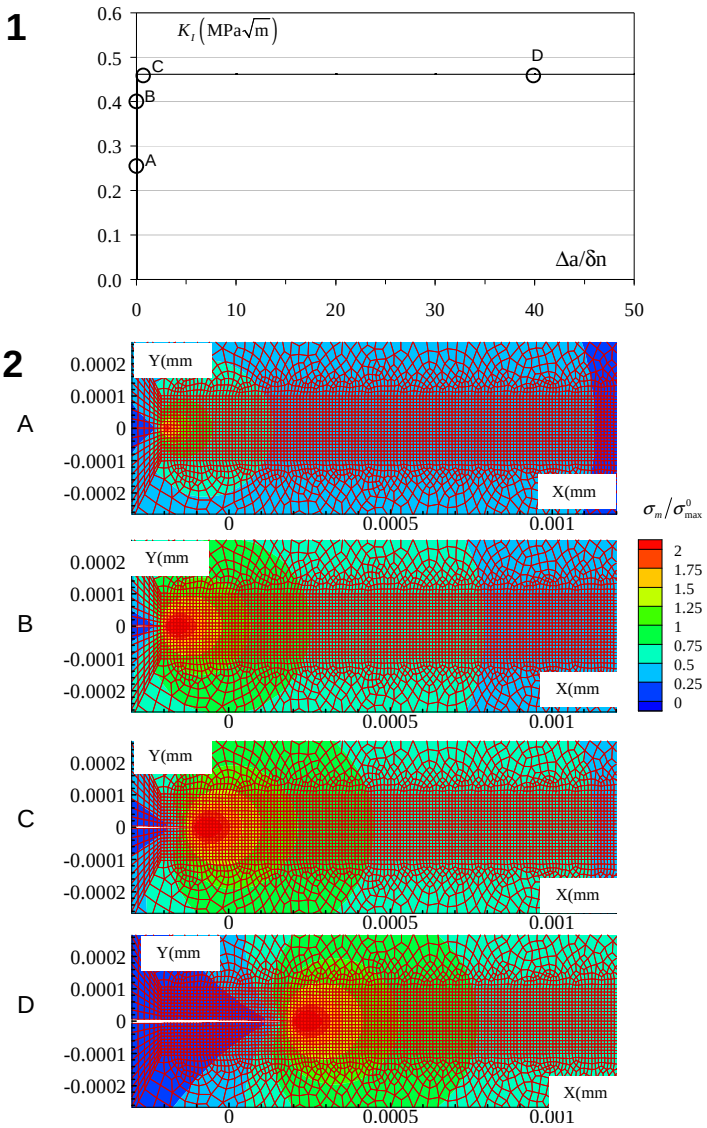

Fig. 2. Homogeneous unbrittled interface, (1) resistance curve with the variation of the applied load in terms of K_I with the crack advance, (2) contour of the mean stress normalized with $\sigma_{max}{}^0$ at stages A, B, C (onset of crack advance) and D (during the crack advance) marked in the plot (1).

taking the Young's modulus E=70 GPa and Poisson's ratio ν=0.3, the theoretical toughness is $K_I^{CR} \approx 0.46\text{MPa}\sqrt{\text{m}}$.

In Fig. 2, we have reported the mean stress distribution at various stages of the crack propagation corresponding to those marked by A, B, C, D of Fig. 1b, for the homogeneous, unbrittled and hydrogen free, interface. The corresponding crack resistance curve is also reported in Fig. 2 where we can observed that the predicted toughness is consistent with the theoretical one. It is worth noting that

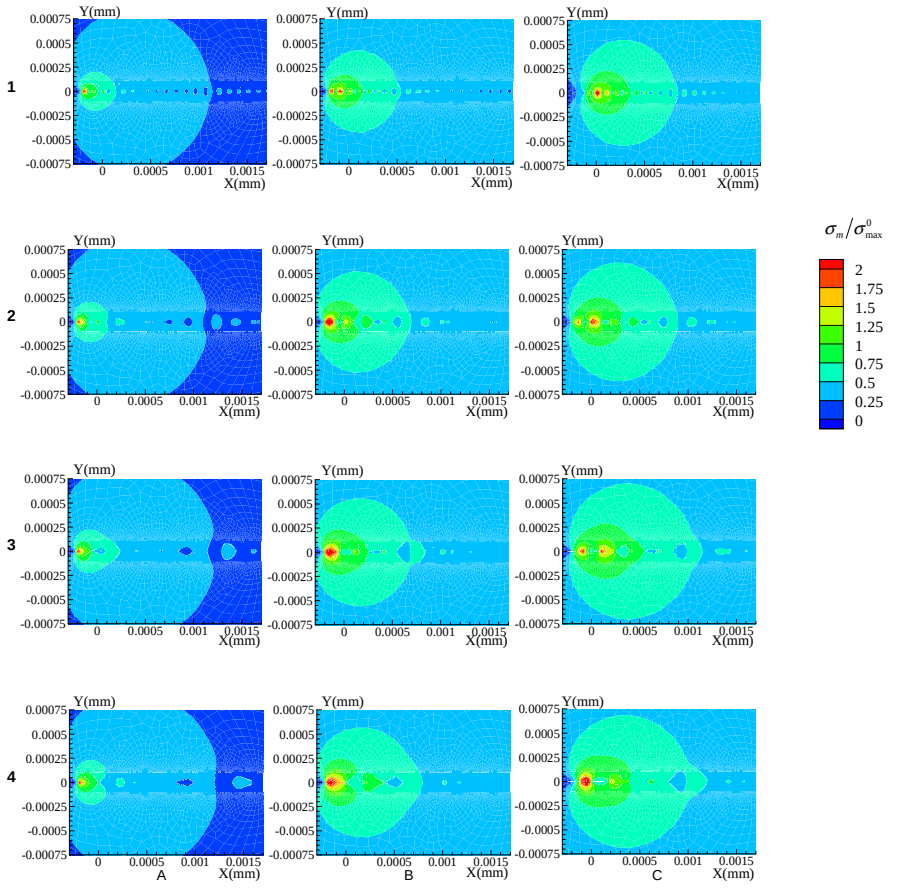

Fig. 3. Contours of the mean stress normalized with $\sigma_{max}{}^0$ peak stress of the unbrittled cohesive zone at stage A, B, C of the cohesive ligament at the crack tip. These distributions correspond to ligaments of (1) 50nm, (2) 100nm, (3) 150 nm and (4) 200nm.

the length of the cohesive zone with non vanishing tractions is about 200nm. This coincides with the range of precipitates and precipitates free ligaments for which a sensibility to hydrogen embrittlement is reported [1].

When a heterogeneous interface is to be considered, the plain/blue zone in Fig. 1a corresponds to the interface with no embrittlement while the dashed/red one corresponds to the weakened. Both have the traction-opening profile reported in Fig. 1b but the maximum traction is different. The ratio between the maximum traction σ_{max} without embrittlement and that weakened due to the presence of H along the interface can be estimated to 1:0.2 from atomistic simulations [4,5]. We have defined the heterogeneous interfaces made of unbrittled and britted zones of equal dimension, with their length ranging from 50nm to 200nm and maximum traction of 1 GPa and 0.2 GPa, keeping δ_n=1nm equal for both zones. At the onset of crack propagation of all cases, the mean stress distribution is reported in Fig. 3.

In the case of an heterogeneous interface of 50nm, 100nm, and also 150nm in Fig. 3a,b and c, at the onset of the crack propagation and related debonding on the unbrittled cohesive zone at the crack tip, the second (and even the third for the case of 50nm long ligaments/precipitates) is already damaged and decohesion has already proceeded. For the case of 200nm long ligaments/precipitates, the picture is somehow similar to that observed for a homogeneous unbrittled interface (Fig.1) with no triggering of decohesion on neighboring ligaments.
These observations result in some assistance in the failure by the heterogeneous nature of the interface for those ranging in 50-150nm and a negligible one for that of 200nm long. Tis is quantified in Fig. 4 in which we have reported the variation of the toughness versus the length of the heterogeneous ligaments/precipitates. With respect to the toughness of the unbrittled, homogeneous interface, we observe in Fig. 4 that the largest embrittlement corresponds to a reduction of the toughness by a factor 0.83. From these variations of the toughness, an estimates of an effective maximum traction σ_{max}^{0} for the decohesion of the heterogeneous interface results in a value σ_{max}^{eff} derived from $\Phi_{SEP} = K_{CR}^2 / E' = \exp(1).\sigma_{max}^{eff}.\delta_n$, in which δ_n remains unchanged while the reduction of the traction at separation $\sigma_{max}^{eff} \approx 0.7\sigma_{max}^{0}$ for the shortest ligaments of 50nm. This value is used latter in the 2D polycrystal analysis for the "effective" cohesive zone and related intergranular failure.

3. On the contribution of the bulk plasticity to in intergranular decohesion

In this section, we sketch the analyses to be performed following the above presented study. We have first focused on the influence of a heterogeneous interface embedded in between two elastic blocks in order to evidence and estimate the contribution of the heterogeneous weakening of the grain boundary on the overall, macroscopic, embrittlement. This analysis is then to be extended with full account of the elastic-plastic response of the surrounding bulk. In particular, we will investigate if damage by the concentration of some plastic deformation locally can be promoted.

4. A 2D polycrystal analysis early stages of crack growth.

Under a small scale yielding analysis, we defined a process zone embedded in an isotropic, elastic-plastic bulk. A regular distribution of grain with cohesive zone along the grain boundaries are considered as depicted in Fig. 4a. The grains have an orientation defined by the Euler angles of the lattice and are prone to fcc crystal viscoplasticity [6, 7]. The effective cohesive zone proposed in the above section is used for the cohesive zones along the grains boundaries. In Fig. 4b, we present a simple simulation representing the crack propagation in an elastic crystal for the purpose of an illustration. Upcoming cases will concerned the influence of the heterogeneous plasticity in the process zone on the crack propagation as well as the influence of initial stresses originated from the process. With the ingredients we consider here, a rate dependence is accounted for through the crystal viscoplasticity only. We first check if that is sufficient to capture slow

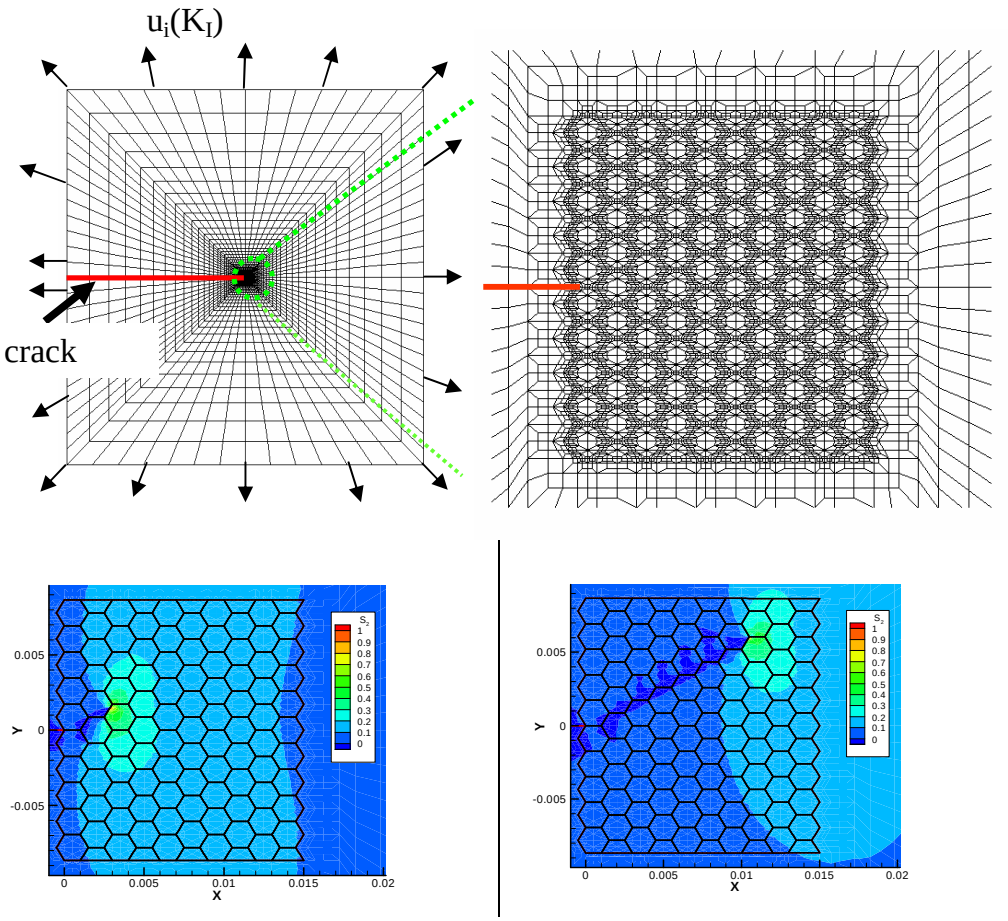

Fig. 4. On the top, schematic description of the loading conditions for the small scale yielding analysis, and zoom in of the 2D-polycrystal process zone. On the bottom, the distribution of the vertical stress component σ_{yy} during the crack propagation for a monotonic loading in an elastic polycristal. Cohesive zones are inserted along each grain boundaries.

crack growth under small loading oscillations around a given load level. This analysis would indicate if a rate dependent formulation of the grain boundary failure is necessary or not to reproduce these observations. The major features governing slow crack growth in a H-precharged samples will then be discussed.

Acknowledgments

The authors gratefully acknowledge the Agence Nationale pour la Recherche under the program ‘HINTER’ and the ‘cluster de recherche MACODEV’ of the Région Rhone Alpes, France for their financial support.

References

[1] R.J. Jones, M.J. Danielson, Role of hydrogen in stress corrosion cracking of low-strength Al-Mg alloys, CORROSION NACE International Conference, Paper 03513, 12 p., 2003.

[2] A. Needleman, Continuum model for void nucleation by decohesion debonding, J. Appl. Mech., Vol. 54 (1987), pp. 525-531.

[3] Xu X.-P., Needleman A., Numerical Simulations of fast crack growth in brittle solids, J. Mech. Phys. Sol., Vol. 42 (1994), pp. 1397-1434.

[4] A. Van der Ven, G. Ceder, The thermodynamics of decohesion, Acta Mater., Vol. 52 (2004), pp. 1223-1235.

[5] S. Serebrinsky, E.A. Carter, M. Ortiz, A quantum-mechanically informed continuum model of hydrogen embrittlement, J. Mech. Phys. Sol., Vol. 52, (2004), pp. 2403-2430.

[6] A. Needleman, R. J. Asaro, J. Lemonds, D. Peirce, Finite element analysis of crystalline solids. Computer Methods in Applied Mechanics and Engineering, Volume 52 (1985), pp. 689-708

[7] D. Peirce, R.J. Asaro, A. Needleman, Material rate dependence and localized deformation in crystalline solids. Volume 31 (1983), pp. 1951-1976